Diavik Waste Rock Project: Thermal Transport in a Covered Waste Rock Test Pile

Nam Pham and David Sego

Department of Civil and Environmental Engineering, University of Alberta, Edmonton, Canada

David Blowes and Richard Amos

Department of Earth and Environmental Sciences, University of Waterloo, Waterloo, Canada

Leslie Smith

Department of Earth and Ocean Sciences, University of British Columbia, Vancouver, Canada

Abstract

Covers are widely used in the management of mine tailings and waste rock and most current cover designs and constructions are in temperate regions. However in cold regions, certain features and processes are unique and they can be utilized to reduce the production of acid rock drainage (ARD). An field study of the thermal behaviour of an experimental covered waste rock pile in a continuous permafrost region is presented. The results indicate that a till unit within the cover remains at sub zero temperatures. The study found that the mean annual heat flux at the base of the layer was significantly less than at the surface due heat retention in the cover and soil saturation levels. The ratio of net radiation to surface heat flux is high and this is common for bare soil surfaces.

Introduction

Mine waste may contain sulphide minerals, such as pyrite and pyrrhotite, and biochemical oxidation of the sulphide minerals can result in acid rock drainage (ARD) if water and oxygen are present. In cold regions, it is well known that cold temperatures can significantly reduce the sulphide oxidation rate. Based on test results from a tailings disposal near Rankin Inlet, Meldrum et al. (2001) suggested that oxidation is significantly reduced at -2 °C due to freezing-point depression of pore water, and was not measurable at -10 °C. Amos et al. (2009) measured oxygen depletion in an experimental covered pile (covered test pile) at Diavik Diamond Mine and calculated an oxidation rate of 10^{-11} kg O_2 m^{-3} s^{-1} at temperatures around 0 °C, which is small compared to other waste rocks typically of $10^{-8} - 10^{-9}$ kg O_2 m^{-3} s^{-1} (Pantelis and Ritchie, 1991). Meanwhile, Elberling (2005) indicated that the temperature that limits on oxidation may be near -5 °C rather than 0 °C.

An insulation cover is used to ensure the frozen waste rock remains frozen and to promote the development of permafrost into unfrozen waste rock. These covers require adequate cold temperatures to maintain mine wastes in a frozen state and a must be sufficiently thick to contain the annual thaw (active layer). The thickness depends on many factors and may range from 1 m to 5 m (MEND1.61.4, 2004). The insulation cover often has a saturated, low permeability layer at the base and a coarse material overlay. The low permeability layer is maintained above 85% saturation via capillary barrier effects and its high moisture content will lower thaw depth via latent heat release. The coarse layer is used to enhance convective cooling (natural convection) during winter. Natural convection has been used to prevent permafrost degradation beneath mine tailings (Arenson and Sego, 2007).

The objectives of this paper are to present temperature data from two vertical thermistor cables and use these measured temperatures to determine thermal properties and heat fluxes within a covered test pile. The test pile is located in a continuous permafrost region at the Diavik Diamond Mine, Northwest Territories, Canada.

Theory

Thermal diffusivity

Conductive heat transport in soils or waste rock is driven by temperature gradients that are typically greater near the ground surface. As a result, cooling and heating rates are also greater near the surface. Temperature oscillations are progressively attenuated and lag with depth due to the thermal diffusivity of the soil. Moreover, nonconductive transport including convection driven by water and air-vapor transport, and phase changes associated with latent heat, also play an important role in highly permeable soils or waste rock. Under the assumptions of a periodically varying soil surface temperature and one-dimensional conductive heat transfer, apparent thermal diffusivity (κ) can be calculated using the phase equation or amplitude equation:

- Phase equation

$$\kappa = \frac{1}{2\omega}\left(\frac{y_2 - y_1}{\delta t}\right) \quad \textbf{(1)}$$

- Amplitude equation

$$\kappa = \frac{\omega}{2}\left(\frac{y_2 - y_1}{\ln\left(\frac{|T_2|}{|T_1|}\right)}\right)^2 \quad \textbf{(2)}$$

where δt is phase difference; $|T_1|$ and $|T_2|$ are the temperature amplitude at two depths y_1 and y_2; ω is the fundamental angular frequency. The phase difference can be obtained using a cross-correlation analysis of two temperature time series (Nakajima and Hayakawa, 1982) and temperature amplitude can be approximated from the minimum and maximum values over a fundamental period of 365 days.

Ground surface heat flux

Measurement or prediction of evaporation is often of great interest in studies of water balance in cover systems. Ground surface heat flux, as a component-of the available energy, is a necessary input for many evaporation measurement and prediction techniques. It is often the smallest component of daily surface energy balance and its magnitude varies with surface cover, soil moisture content, and solar irradiance (Sauer and Horton, 2003). It can reach 300 W m^{-2} for a bare and dry soil in mid summer and drops to less than 20 W m^{-2} for moist soil beneath a plant canopy, residue layer, or snow cover (Sauer and Horton, 2003; Sauer et al., 2003). Ground surface heat flux is determined by using one of four methods: heat flux plate, calorimetric, gradient or a combination of the gradient and calorimetric methods.

The heat flux plate method has been used to study soil heat flux due to the comparative ease of this approach. It was adapted from the efforts to measure heat transfer in walls of buildings and bulkhead of ships (Sauer and Horton, 2003). Soil heat flux plates are small rigid, wafer-shaped sensors that are placed horizontally into the soil. The plate measures the heat flux density which can be correlated to the heat flux density in the soil.

The calorimetric method or temperature integral method determines the average soil heat flux density from the change in heat storage in the soil over a given time interval (Fuchs, 1986).

$$G_{i-1} = D_i C_i \frac{\partial T_i}{\partial t} + G_i \qquad (3)$$

Where G_{i-1} (W m^{-2}) is the heat flux density at the top of a layer i, D_i is the layer thickness (m), C_i (J m^{-3} K^{-1}) is the volumetric heat capacity of the layer, $\frac{\partial T_i}{\partial t}$ (K s^{-1}) is the rate of change of mean temperature of the layer, and G_i is the heat flux at the bottom of the layer. Soil temperature and volumetric heat capacity are the only inputs for completing the heat flux calculations in a calorimetric analysis.

The gradient method is a direct use of $G = -\lambda \frac{\partial T}{\partial t}$. Measured soil temperatures and measured or estimated thermal conductivity, λ, are combined to estimate G. The difficulty of this method is to obtain accurate field values of thermal conductivity (Fuchs, 1986). Soil thermal conductivity changes significantly with water content and temperature (freeze or thaw). This is because of the large differences of thermal conductivities between air and water (ice or liquid water) (Farouki, 1981).

The combined method couples the gradient and calorimetric methods. The gradient method is used to define G at a reference depth, and the calorimetric method is used to determine the heat stored in a layer between the reference depth and the soil surface using (3) (Fuchs, 1986). The need for deep profile measurements of temperature and volumetric heat capacity are avoided.

In this study, the combined method is used to determine surface heat flux at the waste rock surface. Because of its low permeability, the surface heat flux of the cover test pile is based on the conductive heat transfer applied to 0.5 m thick layer at the surface and assuming that temperature profile in this layer is linear (Liang et al., 1999):

$$T = \frac{T_s + T_1}{2} \qquad (4)$$

Using (4) and (3), the surface heat flux G can be described as

$$G = G_1 + \frac{DC}{2\Delta t}\left(T_s^{+} - T_s^{-} + T_1^{+} - T_1^{-}\right) \qquad (5)$$

Where D = 0.5 m and C (J m^{-3} K^{-1}) are the thickness and volumetric heat capacity of the layer, Δt is time between current and previous time step, $T_s^{+}, T_s^{-}, T_1^{+}, T_1^{-}$ are the surface and soil temperature at D depth at the current and previous time step. G_1 is the soil heat flux at the depth D which is calculated base on the temperature of the surface and at depth D.

$$G_1 = \lambda \frac{T_s^{+} - T_1^{+}}{D} \qquad (6)$$

Equation 5 shows that the surface heat flux can be calculated based on thermal properties of the first layer and an assumption of linear temperature variation between the surface and the depth D.

Heat flux through the till cover

In a later section, heat flux is calculated at the bottom of a till layer using five thermistors installed within the till and it is used to predict long term cooling or heating of the material beneath this till layer. A central difference approximation with fourth order error to calculate G_{in} and G_{out} that is in a similar form of (5) is written as (Figure 1):

$$G_{in} = \lambda \frac{T_5 - 8T_4 + 8T_2 - T_1}{12\,D} \qquad (7)$$

$$G_{out} = G_{in} - \frac{2\,DC}{3\Delta t}\left(T_5^+ - T_5^- + T_4^+ - T_4^- + T_3^+ - T_3^-\right) \qquad (8)$$
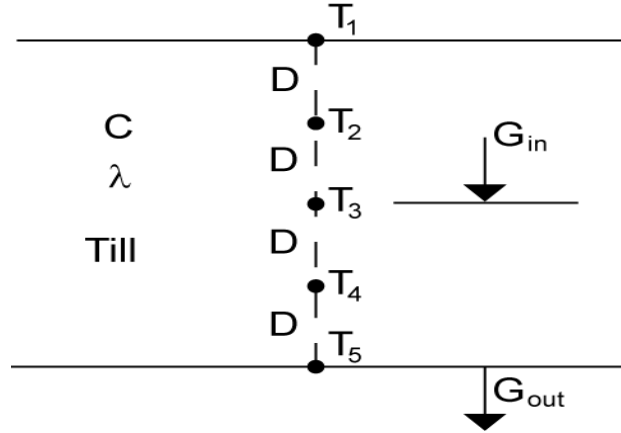

Figure 1: **A schematic for calculation of heat flux at the bottom of till layer**

Site Description and Meteorological Data

Site Description

The Diavik Diamond Mine is located approximately 300 kilometers northeast of Yellowknife, Northwest Territories, Canada. The Arctic Circle is located 220 kilometers north of the mine. The site is located within the continuous permafrost region with an average precipitation of 283 mm with 60% occurring as snow (Neuner, 2009). From 2004 to 2007, three large-scale experimental waste rock piles (test piles) were constructed including the Type I test pile with average sulfur content of < 0.035 wt% S; the Type III test pile with average sulfur content of 0.053 wt % S and the covered test pile with a Type III core, and a 1.5 m till cover overlain by 3 m of the Type I rock (Figure 2). The design concept of the covered test pile is to evaluate the potential to reduce ARD. The lower permeability till layer is intended to maintain a high degree of saturation and therefore reduce oxygen infiltration. The Type I rock layer is intended to contain the active layer. Temperatures measured using the two vertical thermistor cables, C0W5thm and C0E5thm (Figure 2), will be analyzed. More details of construction activities and instrumentation were described by Neuner (2009); Amos et al. (2009); Smith (2009).

Meteorological Data

Based on meteorological data from 2007 to 2010, the monthly average of relative humidity, solar radiation, air temperature, wind speed was calculated. Mean relative humidity was 77 % during the measurement period and monthly average humidity reaches their highest and lowest values in October and June or July each year, respectively (Figure 3A). Meanwhile, monthly average solar radiation reaches a peak of 250 W m^{-2} in mid June and decreases to a minimum of 1.5 W m^{-2} in December (Figure 3B). Measured average air temperatures vary sinusoidally with the coldest temperature in mid January having a monthly average of -29.1 °C and warmest in mid July with an average in July of 11.1 °C (Figure 3C). Furthermore, by averaging over the measuring period, the mean annual air temperature (MAAT) was -9.0 °C and the air temperatures can be simulated using a sinusoidal function of $T_a = -9.0 + 20.1\sin(2\pi t/365)$, in which t is time in days. Wind speed varies significantly and has major

frequencies of 1 day and 14 days. Further, from August to November, wind speed is high with a monthly average of 18.5 km/h and the common winds are northerly to easterly with an average speed of 17 km/h (Figure 3D). Rainfall occurs from May to October annually. During the study period, precipitation reached 153 mm in 2008 that is 93 % of the mean annual precipitation of 164 mm, reported by Environment Canada (2007) in the Lac de Gras area. Meanwhile, the precipitation in 2007, 2009 and 2010 was 93 mm, 73 mm and 95 mm, respectively, which is significant lower than the mean 164 mm (Figure 3E).

Results and Discussion

The surface temperature of the covered test pile and n-factors

The surface temperature of the covered test pile, which is measured within 5 cm of the test pile surface, followed the variation of air temperatures but was warmer (Figure 5A, B; Figure 3C). The average of the mean annual surface temperature (MAST) for the period of measurements was -4.6 °C at C0E5thm and -5.0 °C at C0W5thm. Therefore, the average of MAST of the two thermistor strings was -4.8°C and the amplitude of the mean monthly ground surface temperature was 19.7 °C which is lower than the amplitude of air temperature. The ground surface temperature can be represented by a sinusoidal function of $T_s = -4.8 + 19.7 \sin (2\pi t/365)$. The averaged MAAT over the period of measurements (2007 - 2010) was -9°C. The yearly averaged values were -9.5, -10.0 and -9.6 °C in 2007, 2008 and 2009. However, in 2010, it was an unusually warm winter with MAAT of -6.7°C (Figure 4A). This warm year increased ground temperatures within the test pile. Using the measured air temperatures, air freezing index, I_{af}, the number of negative degree days, is -4335 °C-days and air thawing index, I_{at}, the number of positive degree days, is 1064 °C-days during the measured period. However, in 2010, the values of I_{at} and I_{af} increased to 1188.8 °C-days and -3632.9 °C-days due to the significantly warmer winter (Figure 4B).
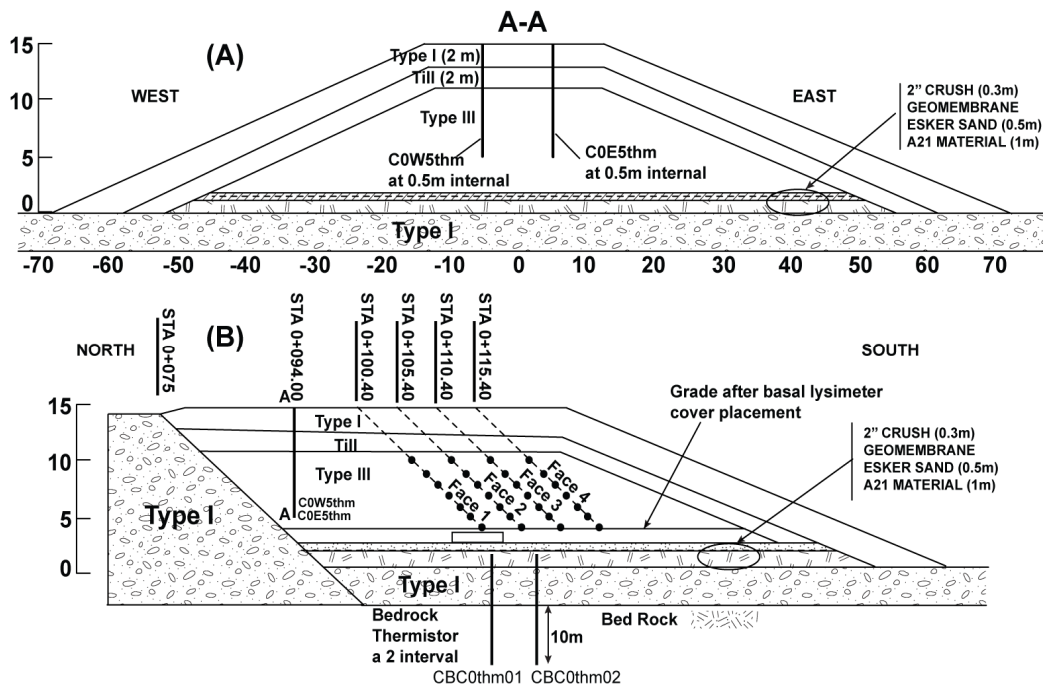

Figure 2: Typical cross-section (A, B) and long section (C) of the covered pile

The difference between values of MAST and MAAT is called the surface offset. The surface offset is a function of the surface energy balance and is controlled by surface characteristics such as vegetation, snow cover, moisture availability and thermal properties of the ground surface (Oke, 1988). The n-factor, a ratio of ground surface freezing or thawing indices to air freezing or thawing indices, is used to represent the surface offset in permafrost conditions (Lunardini, 1978; Jorgenson and Krieg, 1988; Andersland and Ladanyi, 2004). The average ground surface freezing and thawing indices, I_{sf} and I_{st}, of the thermistor cables are -3342 °C-days and 1551 °C-days. The calculated n-factors $n_f = 0.77$ and n_t =1.46 are similar to gravel and concrete pavement type surfaces; $n_f = 0.7 - 0.95$ and $n_t = 1.3\text{-}2.1$ (Andersland and Ladanyi, 2004).

The Figure 6 shows a linear regression of daily average air temperatures against surface temperatures. The regression shows that the daily average surface temperature can be estimated from air temperature through $T_a = T_s - 4.2$ (°C). However, there is considerable spread along the regression line at $T_s < 0$ °C (during winter). This is because the accumulation and redistribution of snow from the top surface to the batter by wind transport changes the surface conditions and thus surface temperatures. Wind speed during the measurement period averaged 17 km h^{-1} with gusts up to 60 km h^{-1}. At these wind speeds, snow depth at the top of the pile was less than 10 cm but the deposition on the batters was between 100 cm to 200 cm (Neuner, 2009).
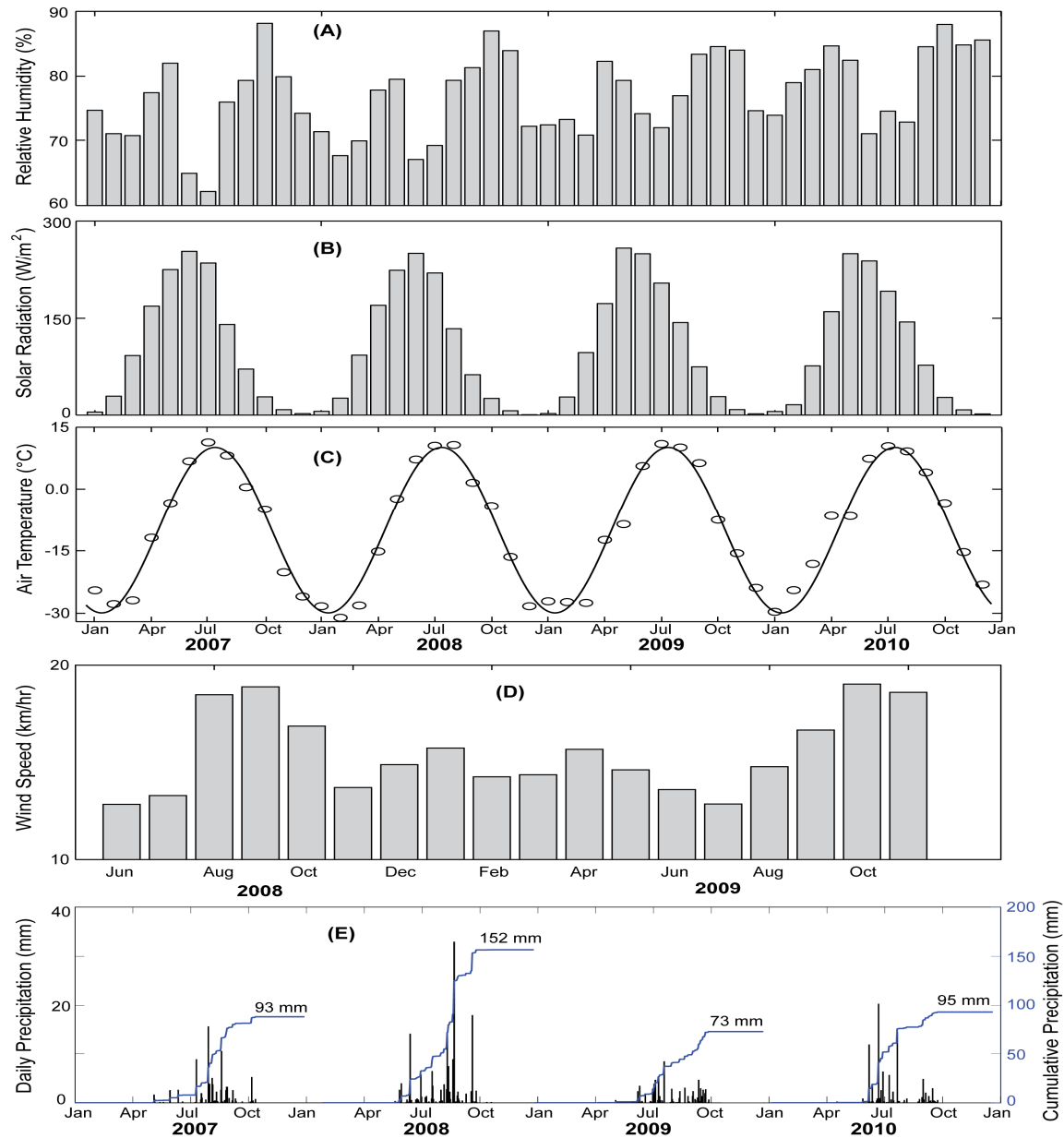
Figure 3: **Meteorlogical data at the test pile research site: Relative Humidity (A), Total Solar Radiation (B), Air Temperature at 10 m from ground surface (C), Wind speed at 10 m (D) and Daily Precipitation (E).**

Ground surface temperature

The fluctuation of the surface temperature of the covered test pile changes temperatures at depth but with smaller means and amplitudes depending on the distance from the surface. At a depth of 0.5 m, the mean monthly ground temperature (average of C0E5thm and C0W5thm over the period of measurements) reached a maximum value of 10.2 °C in August and decreased to a minimum value of -18.2°C in mid February. The mean annual ground temperature and amplitude at this depth were -4.0 °C and 14.2 °C (Figure 5). At depths of 3.0 m and 4.5 m, the ground temperatures varied with much smaller amplitudes; 8.3°C (between 0 °C and -8.3 °C) at the 3.0 m depth and 5.7 °C (between 0 °C and -5.7 °C) at 4.5 m depth in winters 2008 and 2009 (Figure 5). However, due to significant warmer

weather in winter 2010, the amplitudes dropped to 6.7 °C and 4.5 °C at depths of 3.0 m and 4.5 m respectively. At 10 m depth, the ground temperature varied with an insignificantly small amplitude of 1.6°C (between 0.2°C and -1.4°C) and showed a small change in temperatures due to the warmer 2010.

Active layer

The active layer in a permafrost region consists of the depth to which ground temperatures fluctuate above and below 0 °C during the year. The thickness of this layer depends on air temperatures and ground surface conditions such as: snow, moisture content, vegetation, drainage, and the orientation of the surface (Andersland and Ladanyi, 2004). Based on monthly average temperatures, temperature profiles were plotted in the representative years, 2008 and 2009 (Figure 7). The two thermistor strings show almost identical results and indicate the active layer stays within the Type I rock that is about 2 m thick. At the top of the till layer temperatures varied between 0 °C and -12.2 °C (Figure 7) and at the base temperatures varied between 0 °C and -8.2 °C. The temperatures within the till stay below 0°C year round, whereas the temperatures above the till vary with the season. In June to October each year there were some portions of the Type I layer increase to above 0°C, but the rest of the year the entire profiles were below 0°C (Figure 7).

Thermal properties

Thermal diffusivities of the test pile layers were determined by using a time series of temperatures at depths. The time lag and amplitude damping between surface and internal temperatures of the test pile show three distinct regions corresponding to Type I rock, till and Type III rock (Figure 8). The averaged-calculated thermal diffusivities of Type I rock, till and Type III rock are 6.72×10^{-7} m^2 s^{-1}, 1.53×10^{-6} m^2 s^{-1} and 7.96×10^{-7} m^2 s^{-1} respectively. The calculated thermal diffusivity values by (1) or (2) give slightly different results (

Table). Below a depth of 2 m, temperatures are below 0 °C, therefore, the calculated thermal diffusivity of the till and Type III rocks are for frozen materials. Meanwhile, the calculated thermal diffusivity of the Type I rock is in the range of these frozen and thawed values. This range should be small due to its low moisture content and is also indicated through an insignificant change of in-situ measured thermal conductivities of Type I or III rock materials in the frozen or thawed state. Further, the thermal diffusivity of the till is higher due to its high moisture content, low void ratio and frozen condition. The calculated thermal diffusivity from Type I rock temperatures is quite comparable with calculated thermal diffusivity from measured thermal conductivity of 6.72×10^{-7} m^2 s^{-1} measured in waste rock piles at Aitik, Sweden (Tan and Ritchie, 1997). Tan and Ritchie (1997) also commented on the consistency of calculated thermal diffusivity from measured thermal conductivity and from measured temperature profiles at the same location. The low moisture content makes measured thermal conductivity insensitive to temperatures and the average over five years (from 2006 to 2010) of field measured thermal conductivity was 1.65 W m^{-1} K^{-1} for the Type I rock and 1.69 W m^{-1} K^{-1} for the Type III rock. Therefore, the bulk volumetric heat capacities which are calculated through thermal conductivities and thermal diffusivities of the Type I and Type III rock are 2.38×10^6 J m^{-3} K^{-1} and 2.13×10^6 J m^{-3} K^{-1} respectively.

The till material is below 0 °C year round and the averaged bulk density of the till is 2180 kg m^{-3}. In addition, the void ratio is 0.20 and the averaged initial water content is 17 % (correspond to 90 % degree of saturation). Assuming that the specific heat capacity of the solid phase (granite) is 790 kJ kg^{-1} K^{-1} (Tan and Ritchie, 1997), the bulk volumetric heat capacity of till (through volume average of each component) in the frozen state is $2108*(790*0.8+2050*0.17+0.03*1005) = 2.13 \times 10^6$ J m^{-3} K^{-1}. As a result, the frozen thermal conductivity of the till is $2.13 \times 10^6 * 1.53 \times 10^{-6} = 3.26$ W m^{-1} K^{-1} which is similar to values used in numerical simulations for frozen glacial till conducted by AMEC (2007) and Pimentel et al. (2011).
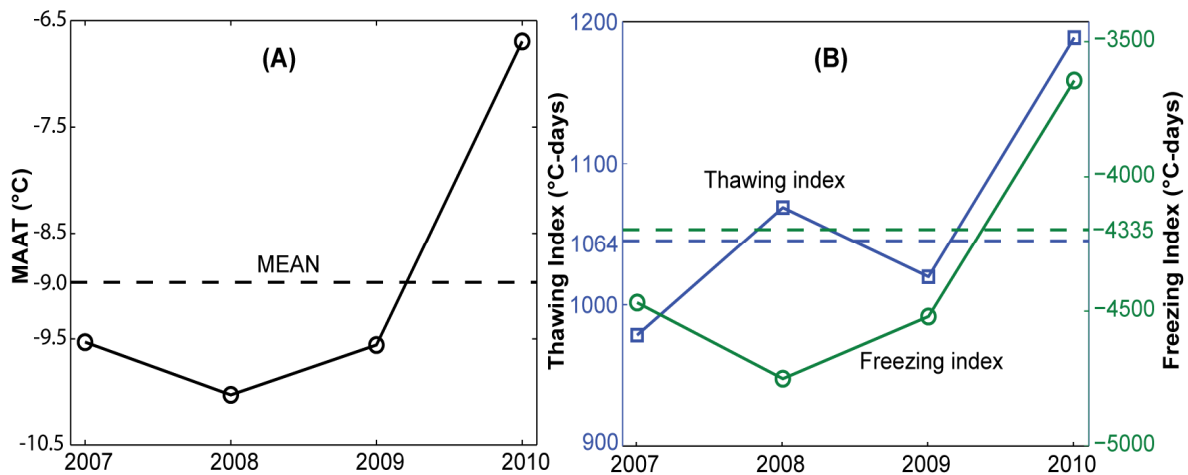

Figure 4: MAAT (A) and calculated thawing and freezing indices (B).

Net radiation and heat fluxes

The detail of the calculation of net radiation are not shown in this paper but are based on the meteorlogical data (Figure 3), surface temperatures of the pile and an averaged-measured cloud cover of 68 %. Monthly average of net radiation varied sinusoidally and reached a maximum value of 96.5 W m^{-2} in July and minimum value of -69.7 W m^{-2} in mid December. The net radiation values can be fitted using a sinusoidal function $R_n = 13.4 + 83.1\sin(2\pi t/365 - 1.30)$, with the mean annual net radiation of 13.4 W m^{-2} (Figure 9A).

The surface heat flux of the test pile was calculated using equation 5 and the previously presented thermal properties. Similar to the net radiation, the calculated monthly averaged surface heat flux fluctuates sinusoidally between 20.4 W m^{-2} in July and -28.6 W m^{-2} in mid December annually (Figure 9A). The fitting curve of the surface heat flux is G = -4.1 + 24.5sin(2πt/365 - 1.35) with the mean annual surface heat flux of -4.1 W m^{-2}. Net radiation and surface heat flux are only positive between April and August annually, which means that during this period, heat enters the test pile. The ratio between the mean net radiation and mean surface heat flux is 0.31 and this value is common for bare soil surfaces, which range from 0.22 to 0.51, depending on soil moisture content at the surface (the higher the moisture content, the lower the ratio) (Idso et al., 1975).

The heat exchange between the bottom of the till layer and the ambient environment is low due to the high moisture content, low permeability and frozen state of the till, as well as its distance from the surface. Heat flux across the bottom of the till was calculated using five thermistors within the till and equation 8. The monthly averaged magnitude of heat flux across the bottom of the till from June to December was around 1.2 W m^{-2} annually which is about 5.9 % of monthly averaged magnitude of surface heat flux in summer (Figure 9B). From December to June, the heat flux was negative and reached a peak of -5.8 W m^{-2} (averaged over 3 winters). Moreover, the mean annual heat flux across the bottom of the till was -1.78 W m^{-2} which is 43 % of mean annual surface heat flux. The amplitude of heat flux at the bottom of the till is much lower than heat flux at the surface of the test pile. The mean annual heat flux at the surface and at the bottom of the till was negative and indicates the covered test pile is cooling.
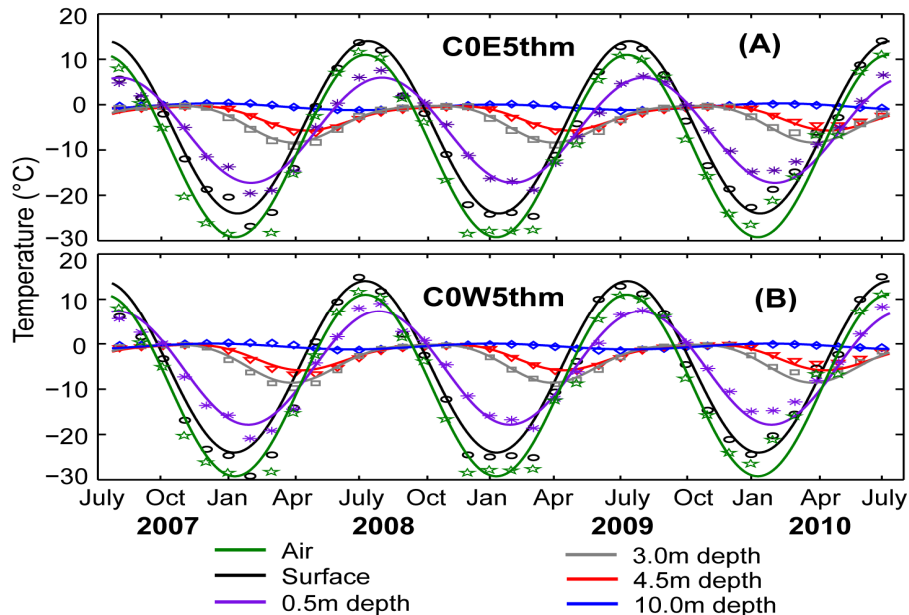

Figure 5:   **Monthly ground temperatures at   selected depths of the thermistor cables C0E5thm (A) and C0E5thm (B).**
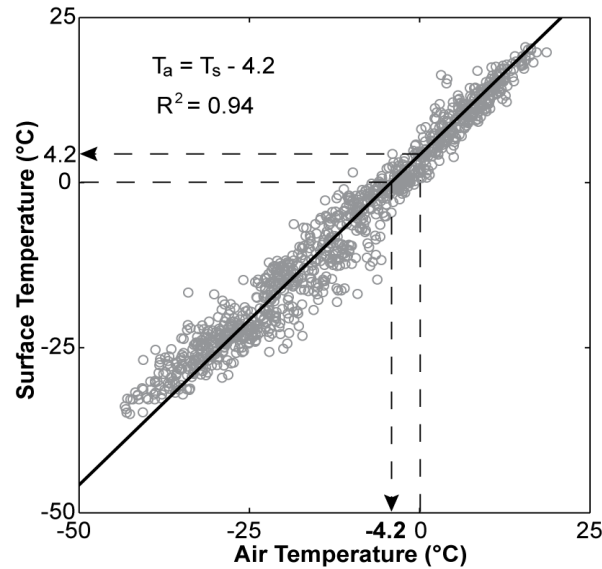
Figure 6:   Daily averaged surface versus air temperature.

Conclusions

Temperature measurements of an experimental covered water rock pile constructed in a continuous permafrost region were presented. The MAAT and MAST between 2007 and 2010 was -9.0 °C and -4.8 °C and using daily averages, a linear regression between air temperature and the pile's surface temperature is $T_a = T_s - 4.2$ (°C). In addition, surface conditions of the experimental pile are represented through n-factors $n_f = 0.77$ and $n_t = 1.46$. Ground temperatures in the Type I rock above the till layer fluctuate with air temperature but at smaller amplitudes. The Type III rock temperatures were below 0 °C and vary at insignificant amplitudes compared to air temperature due to the higher moisture content of the till layer. Further the active layer is contained in the Type I rock layer as expected. Based on measured temperatures and thermal conductivities, the other thermal properties were calculated. The thermal conductivities of the Type I, till and Type III rock are 1.65, 3.26, 1.69 W m^{-1} K^{-1}, respectively, and the bulk volumetric heat capacities of the Type I, till and Type III rock are 2.38×10^6, 2.13×10^6, and 2.13×10^6 J m^{-3} K^{-1}, respectively.

Net radiation varied significantly through the year between 96.5 W m^{-2} and -69.7 W m^{-2}, whereas surface heat flux had a smaller amplitude between 20.4 W m^{-2} and -28.6 W m^{-2}. Further, the ratio between the net radiation and surface heat flux was 0.31. The mean annual heat flux through the bottom of the till was -1.78 W m^{-2} which is 43 % of mean annual surface heat flux.

Acknowledgements

References

AMEC (2007). *A21 DIKE: Final Design Report: Volume I.* Prepared for Diavik Diamond Mines Inc. Yellowknife, Northwest Territories.

Amos, R. T., Smith, L., Neuner, M., Gupton, M., Blowes, D. W., Smith, L., and Sego, D. C. (2009b). Diavik waste *rock project: Oxygen transport in covered and uncovered piles. In The 8th ICARD International Conference On Acid Rock Drainage, Skelleftea, Sweden, 2009.*

Andersland, O. B. and Ladanyi, B. (2004). Frozen Ground Engineering. John Wiley & Sons.

Arenson, L. and Sego, D. (2007). Protection of mine waste tailing ponds using cold air convection. *Assessment and Remediation of Contaminated Sites in Arctic and Cold Climates*.

Elberling, B. (2005). Temperature and oxygen control on pyrite oxidation in frozen mine tailings. *Cold Regions Science and Technology*, 41(2):121-133.

Environment Canada (2007). *Climate Data Online 2002-2007*, National Climate Data and Information

Archive, <http://climate.weatheroffice.ec.gc.ca/climateData/canada_e.html>.

Farouki, O. T. (1981). *Thermal properties of soils*. United States Army Corps of Engineers, Cold Regions Research and Engineering Laboratory, Hanover, New Hampshire, USA.

Fuchs, M. (1986). *Methods of soil analysis. Part I. Physical and mineralogical methods. SSSA Book Series no5. SSSA, Madison, WI.*

Idso, S. B., Aase, J. K., and Jackson, R. D. (1975). Net radiation - soil heat flux relations as influenced by soil water content variations. *Boundary-Layer Meteorology*, 9:113-122.

Liang, X., Wood, E. F., and Lettenmaier, D. P. (1999). Modeling ground heat flux in land surface parameterization schemes. *J. Geophys. Res.*, 104(D8):9581-9600.

Lunardini, V. (1978). Theory of n-factors and correlation of data. *In The 3rd International Conference on Permafrost*, pages 41-46. National Research Council of Canada, Ottawa.

MEND1.61.4 (2004). Covers for reactive tailings in permafrost regions. Technical report, *The Mining Associationof Canada-Mine Environment Neutral Drainage (MEND) Program.*

Moncur, M., Ptacek, C., Blowes, D., and Jambor, J. (2005). Release, transport and attenuation of metals from an old tailings impoundment. *Applied Geochemistry*, 20(3):639-659.

Neuner, M. (2009). *Water flow through unsaturated mine waste rock in a region of permafrost.* M.Sc. thesis, The University of British Columbia.

Pantelis, G. and Ritchie, A. I. M. (1991). Macroscopic transport mechanisms as a rate-limiting factor in dump leaching of pyritic ores. *Applied Mathematical Modeling*, 15(3):136-143.

Sauer, T. and Horton, R. (2003). *Soil heat flux. In Micrometeorological measurements in agricultural systems*. ASA Monograph. American Society of Agronomy, Madison, WI.

Smith, L. J. D. (2009). *Building and characterizing low sulfide instrumented waste rock piles: Pile design and construction, particle size and sulfur characterization, and initial geochemical response*. M.Sc. thesis, University of Waterloo.
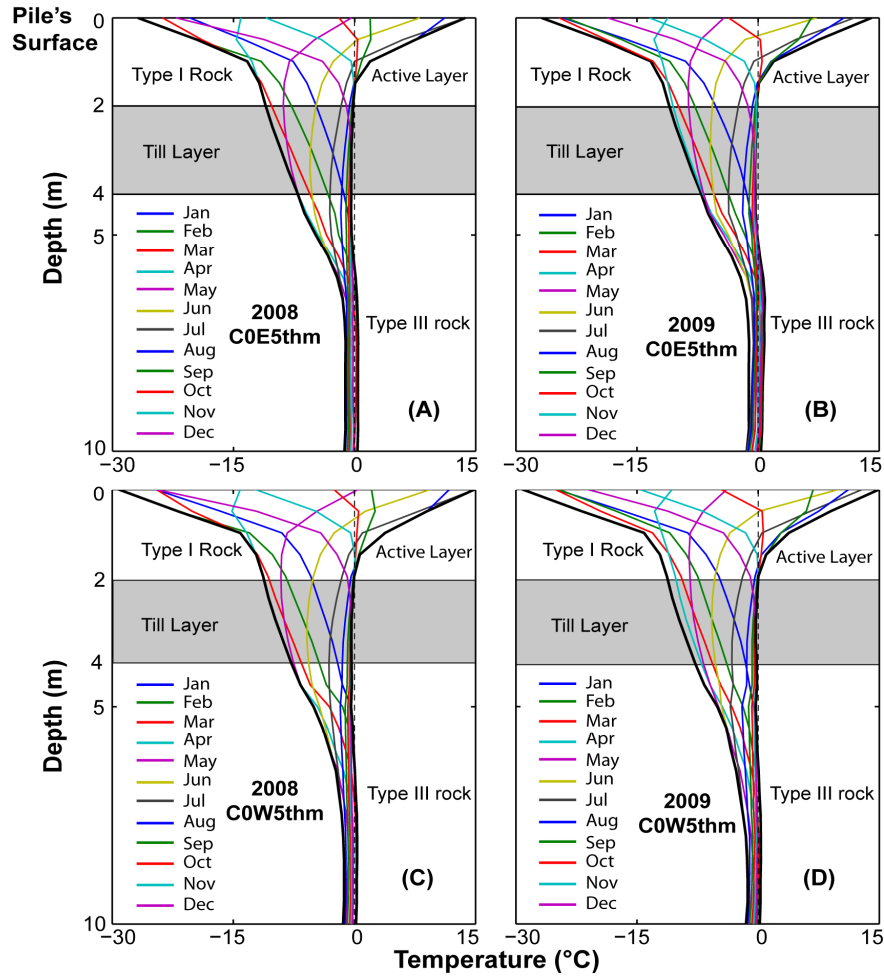
Figure 7: **Temperature profiles (monthly averaged) of thermistor string C0E5thm in 2008 (A) and 2009 (B), and thermistor string C0E5thm in 2008 (C) and 2009 (D).**

Table 1: **Calculated thermal diffusivities ($m^2\ s^{-1}$)**

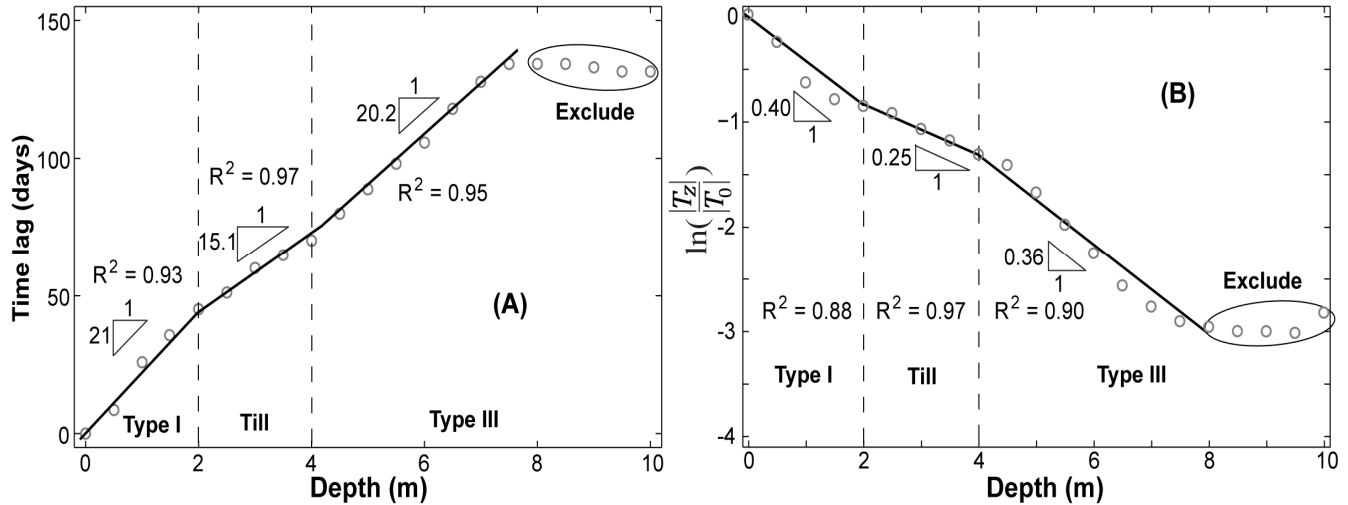|	Time lag by (1)	Amplitude damping by (2)	Averaged
Type I rock	7.62×10^{-7}	6.23×10^{-6}	6.92×10^{-7}
Till	1.47×10^{-6}	1.59×10^{-6}	1.53×10^{-6}
Type III rock	8.24×10^{-7}	7.69×10^{-7}	7.96×10^{-7}

Figure 8: **Plot of time lag (A) and natural logarithm of amplitude ratio (B) versus depths.**
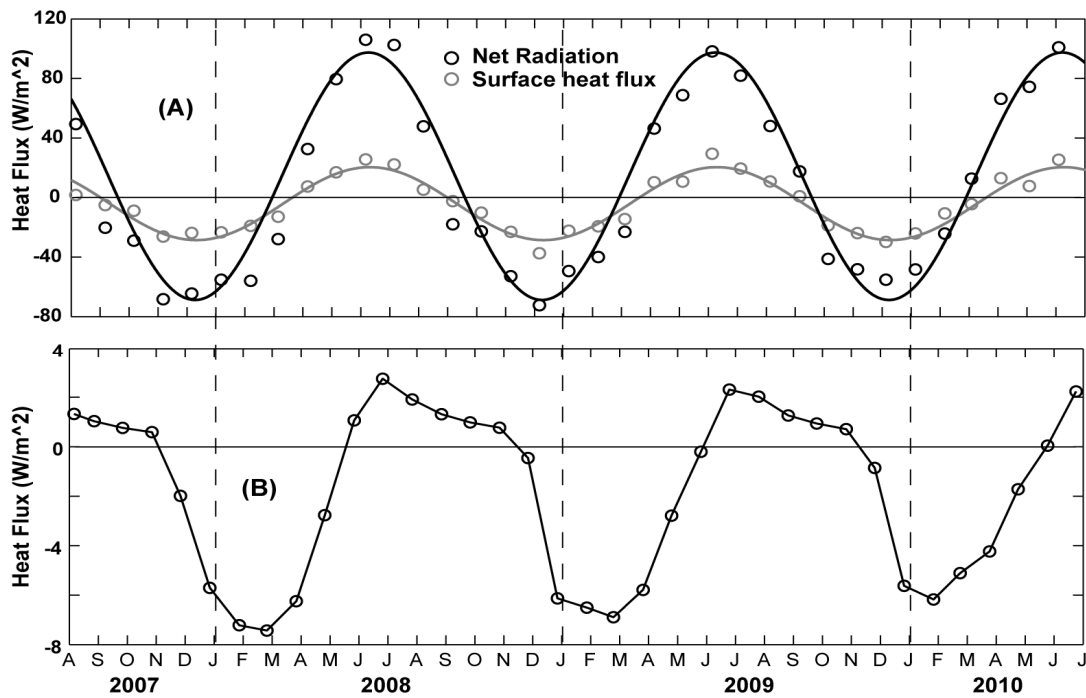

Figure 9: **Monthly averaged of net radiation and surface heat flux (A) and heat flux across the bottom of the till layer (B).**